scientific reports

OPEN

Effect of inoculation dose on infection kinetics and immune responses to *Giardia*

Bregt Decorte✉, Charlotte E. Van Crombrugge & Peter Geldhof

Giardia duodenalis is a globally prevalent enteric parasite capable of establishing both acute and chronic infections. While infection dose is known to influence early infection dynamics, its effect on immune activation and chronicity remains poorly defined. In this study, we investigated how varying inoculum sizes affect infection kinetics and immune development in both immunocompetent (C57BL/6J) and T cell–deficient (TKO) mice. High infection doses induced earlier cyst shedding and accelerated interleukin-17A (IL-17) responses, while lower infection doses resulted in delayed immune activation. Despite these early differences, cumulative cyst excretion and clearance kinetics eventually converged across dose groups. In TKO mice, infection was not controlled regardless of dose, yet parasite loads plateaued, suggesting host-intrinsic limits to expansion. Longitudinal follow-up in C57BL/6J mice revealed persistent low-level infection and sustained upregulation of IL-17A, mannose-binding lectin 2 (Mbl-2) and inducible nitric oxide synthase (NOS2) up to six months post-infection, despite low trophozoite counts. These findings confirm a central role for IL-17A in anti-giardial immunity and suggest that infection dose modulates the timing but not the outcome of immune control. Persistent IL-17A signaling during chronic infection may contribute to long-term host-pathogen interactions, with potential implications for intestinal health and secondary pathogen resistance.

Keywords *Giardia*, Infection dose, Infection dynamics, Chronic, Immunity, IL-17A

Giardia duodenalis (syn. *G. intestinalis*, *G. lamblia*) is a flagellated protozoan parasite and one of the most common intestinal pathogens worldwide. It infects humans as well as a broad range of domestic and wild animal species[1]. The parasite has a simple and direct life cycle. Infection occurs by the ingestion of environmentally resistant cysts, typically through contaminated food or water. After passage through the stomach, cysts excyst in the duodenum to form an excyzoite that undergoes successive divisions to produce four trophozoites[2]. These trophozoites do not invade host cells but instead attach to the intestinal mucosa. Within the intestinal lumen, they multiply rapidly through binary fission. In response to environmental signals, such as altered pH or bile concentration, trophozoites encyst, forming new cysts that are shed in the feces, thus completing the life cycle[3].

Clinical manifestations of giardiasis range from asymptomatic carriage to gastrointestinal illness, commonly presenting with diarrhea, abdominal discomfort, nausea, weight loss and impaired growth, particularly in young or immunocompromised hosts[4]. While many infections are self-limiting, a subset progresses to chronicity, with symptoms persisting for weeks or months[5,6]. Chronic giardiasis has been documented across species, including humans[7], dogs[8], cattle[9] and mice. In mice, intestinal trophozoite colonization has been observed up to three months post-infection[10].

The development of chronic infections is likely multifactorial, involving both host and parasite determinants. Host-related factors, such as age, sex, immune competence, prior exposure, diet and gut microbiota composition may influence susceptibility and disease course[11,12]. Parasite-specific traits, including genotype, replication rate, expression of variable surface proteins, immune evasion and drug resistance also contribute to persistence[6]. Chronic giardiasis is sometimes accompanied by diarrhea and intestinal malabsorption, leading to nutrient deficiencies such as lactase, vitamin A, B_{12}, and folate[13]. Notably, parasite clearance does not always equate to clinical recovery; some patients continue to experience gastrointestinal symptoms following treatment, especially after chronic or treatment-refractory infections, suggesting long-lasting physiological alterations[14]. Interestingly, several epidemiological studies have reported an inverse association between *Giardia* infection and the incidence of moderate-to-severe diarrhea in children living in endemic regions[15–18]. These findings contrast with the established pathogenic role of *Giardia*, suggesting that under certain conditions colonization may exert

Laboratory of Parasitology, Department of Translational Physiology, Infectiology and Public Health, Faculty of Veterinary Medicine, Ghent University, Merelbeke 9820, Belgium. ✉email: Bregt.Decorte@UGent.be

a protective or modulatory effect on gut physiology or the microbiota. However, the mechanisms underlying this potential protection remain unclear. This paradox highlights the complexity of host-parasite interactions and the importance of host immune responses in shaping infection outcomes.

Recent studies have firmly established IL-17A as a critical cytokine in the immune response against *Giardia* infections. During a *Giardia* infection, IL-17A is primarily produced by T helper 17 (Th17) cells residing in the lamina propria of SI[19,20], where it orchestrates multiple protective mechanisms. These include the upregulation of antimicrobial peptides such as angiogenin-4 (Ang-4) and α/β-defensins[19,21], promotion of complement activation via Mbl-2[22–24] and enhanced transport of IgA into the intestinal lumen through increased expression of the polymeric immunoglobulin receptor (pIgR)[19,23]. The importance of IL-17A is highlighted by the fact that mice lacking T cells (TKO mice) are unable to resolve infection within the typical three-week period, demonstrating that T cell-mediated immunity is essential for parasite clearance[19,20,25–27].

Infection dynamics are also influenced by the infective dose. Early studies in murine models of *G. muris* demonstrated that higher inocula accelerate the onset of cyst excretion and may impair host weight gain, while peak cyst output appeared largely independent of the initial dose[28–30]. However, these foundational investigations were restricted to short-term outcomes and preceded the recognition of IL-17A as a pivotal cytokine in anti-giardial immunity. This study aimed to elucidate how the initial *Giardia* infection dose influences the trajectory of infection and associated immune responses in a murine infection model. Using both immunocompetent C57BL/6J mice and TKO mice, we assessed the kinetics of parasite excretion and mucosal immune activation across varying inocula. Focus was placed on IL-17A-mediated responses, as they are central to *Giardia* immunity. By extending the observation period into the chronic phase of infection, this work provides novel insights into the long-term interplay between parasite burden, host immune competence and sustained cytokine expression.

Results

Initial infection dose shapes early infection kinetics and the intestinal IL-17A response in *Giardia*-infected C57BL/6J mice

To investigate the impact of infection dose on the course of *G. muris* infection in immunocompetent mice, six-week old female C57BL/6J mice were inoculated with varying doses of *G. muris* cysts (infection study 1). Fifteen mice were assigned to receive one of four infection doses—10^2, 10^3, 10^4 or 10^5 cysts—referred to as doses 1 through 4, respectively. Cyst excretion was monitored throughout the 21-day study period (Fig. 1a). Mice receiving higher doses (doses 3 and 4) exhibited an earlier and more pronounced peak in cyst shedding, around day 5–7 post infection (p.i.), followed by a sharp decline by day 12 p.i.. In contrast, mice inoculated with lower doses (doses 1 and 2) demonstrated a delayed and lower peak excretion, but cyst shedding persisted for a longer duration. Cumulative cyst excretion, expressed as cumulative cysts per gram (CCPG), was compared between the groups over time (Fig. 1b). Between days 0 and 7 p.i., CCPG was significantly higher in mice receiving doses 3 and 4 compared to those in the lower dose groups (doses 1 and 2), reflecting the accelerated onset of infection in the higher inoculum groups. However, these differences had diminished and were no longer significant by day 14 p.i.. By day 21 p.i., CCPG values were comparable across all infection doses. Total intestinal trophozoite counts (TCs) were assessed on days 7, 14, and 21 p.i. (Fig. 2). On day 7 p.i., TCs were significantly lower in the lowest dose group compared to the other groups, with the highest counts observed in mice inoculated with dose 2. By day 14 p.i., TCs had decreased in all groups except group 1, where counts had increased compared to day 7. By day 21 p.i., TC values were uniformly low across all groups, with no significant differences between them, indicating effective control of infection by the host in all groups.

To elucidate the host immune response, expression levels of IL-17A and its downstream effector Mbl-2 were quantified in the SI, Peyer's patches (PP) and mesenteric lymph nodes (MLN) at days 7, 14, and 21 p.i.. In the SI (Fig. 3), IL-17A expression was dose- and time-dependent. On day 7 p.i., IL-17A expression was lowest in dose group 1, while significantly upregulated in dose groups 2 and 4, compared to uninfected control mice. Mice in dose group 3 showed a trend toward increased IL-17A, although this did not reach statistical significance. By day 14 p.i., IL-17A was significantly upregulated in dose groups 1 and 2, but no longer significantly elevated in dose group 4 compared to uninfected controls. At day 21 p.i., expression levels were comparable across all groups, though still significantly elevated in doses 3 and 4 compared to controls. Mbl-2 expression in the SI showed a similar dynamic. At day 7 p.i., it was significantly upregulated in doses 2–4 compared to uninfected controls, but not in dose 1. By day 14 p.i., expression became more uniform across groups, with significant upregulation in doses 1–3. At day 21 p.i., expression remained consistent among groups, with significant upregulation in doses 1, 3, and 4. In contrast, the PP showed no significant IL-17A upregulation at any time point. However, Mbl-2 expression was significantly elevated in doses 3 and 4 on days 7 and 21 p.i., and in doses 1 and 4 on day 14 p.i. (**Supplementary Fig. S1**). No increased IL-17A expression was detectable in the MLN at any time point after infection in all dose groups (**Supplementary Fig. S2**).

Throughout the course of the study, body weight was monitored to serve as an indicator of overall health (Fig. 4). In the lower dose groups (doses 1–3), significant reductions in weight gain were observed compared to uninfected controls. Intriguingly, mice in the highest infection dose group gained the same amount of weight as uninfected controls. **Supplementary Table S1** further details the average body weights at all weighing points for control mice and *G. muris*-infected mice across the different infection doses.

Parasite burden in TKO mice reaches a plateau within 2 weeks after *Giardia* infection regardless of the initial infection dose

As immunocompetent mice all controlled the infection within 3 weeks regardless of their initial infection dose, we next investigated how *Giardia* infection unfolds in the absence of adaptive immunity. To this end, a dose-response experiment was conducted in TKO mice, which lack the ability to mount an effective immune response against *Giardia*[19,27]. The objective was to assess whether parasite load, measured by cyst excretion and
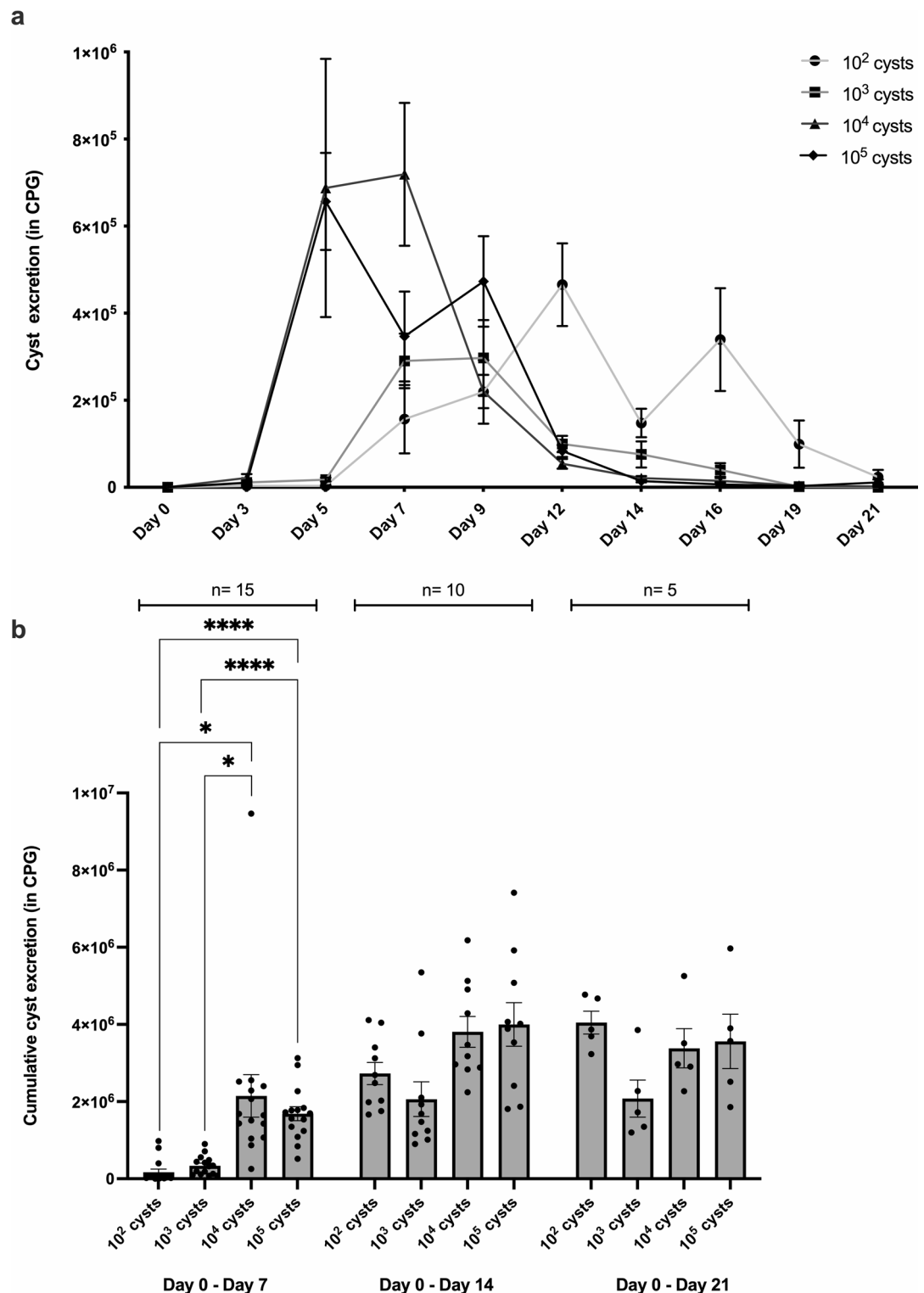
Fig. 1. Dose-dependent effects of *G. muris* infection on cyst excretion dynamics in C57BL/6J mice. (**a**) Fecal cyst counts were monitored every 2–3 days up to day 21 p.i.. Each point represents the mean number of cysts per gram of feces (CPG) ± SEM ($n = 15$ for days 0–6; $n = 10$ for days 8–13; $n = 5$ for days 15–21). (**b**) Cumulative fecal cyst output (CPG) calculated over three time-intervals: days 0–7, 0–14, and 0–21 p.i.. Each bar represents the mean cumulative cyst count ± SEM (same n as above for each interval). Differences were analyzed using a mixed-effects model with Bonferroni correction for multiple comparisons (*$P < 0.05$, ****$P < 0.0001$).
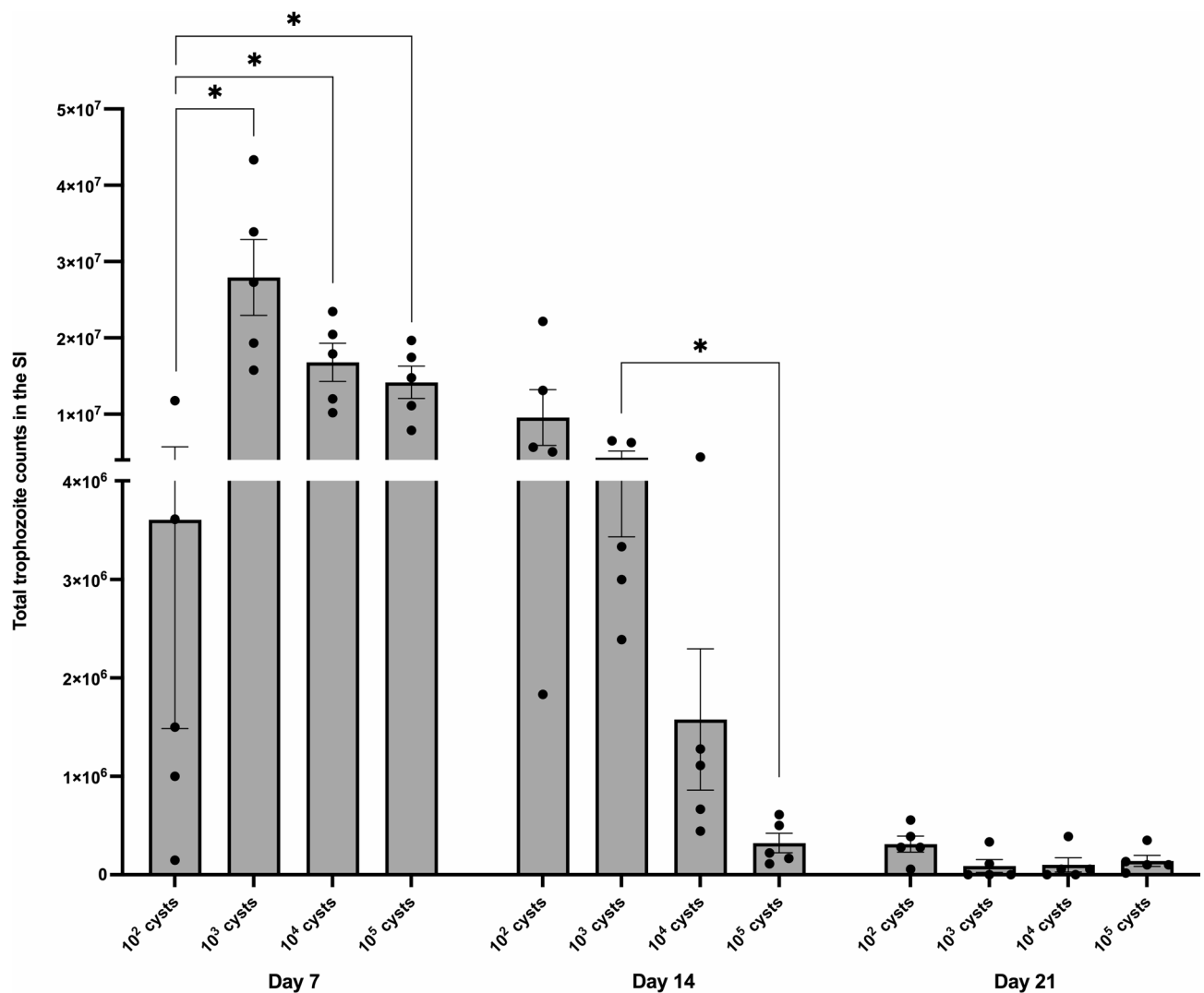
Fig. 2. Dose-dependent effects of *G. muris* infection on intestinal trophozoite burden in C57BL/6J mice. Total small intestinal trophozoite counts were quantified at days 7, 14, and 21 p.i. for each infection dose group ($n = 5$ per time point per group). Bars represent mean values ± SEM. Differences between groups were analyzed using a Kruskal–Wallis test (*$P < 0.05$).

trophozoite counts, would still reach an upper threshold in the absence of immune control, due to possible host-related factors, such as limited nutrients within the intestinal environment or physical limitations on the intestinal epithelium that restrict further increases in parasite burden. Five six-week old female TKO mice per group were infected with either 10^2 (low dose) or 10^4 (high dose) *G. muris* cysts and cyst excretion was monitored over a 31-day period (infection study 2). On the last day of the study, the mice were euthanized for quantification of trophozoites in the SI. Mice in the high-dose group exhibited an earlier and more pronounced peak in fecal cyst shedding, occurring around day 7 p.i. (Fig. 5a). However, by day 12 p.i., cyst excretion levels converged between the two groups and remained comparable for the remainder of the study. Similarly, TCs were nearly identical across the 2 groups at day 31 p.i., indicating that parasite loads were unaffected by the initial infection dose (Fig. 5b).

### Sustained IL-17A expression and immune activation during chronic *Giardia* infection in C57BL/6J mice

To investigate the chronic phase of infection in both immunocompetent and immunodeficient mice, a 6-month longitudinal infection study was conducted in C57BL/6J and TKO mice (infection study 3). Six-week old female C57BL/6J and TKO mice were inoculated with 10^3 *G. muris* cysts and fecal cyst counts and TCs were monitored throughout the course of the study. In C57BL/6J mice, cyst excretion peaked around day 7 p.i. and subsequently declined to low but persistent levels that continued throughout the 6-month study period. In contrast, TKO mice exhibited persistently high levels of cyst excretion (Fig. 6). TCs were assessed at 2, 4, and 6 months p.i. (Fig. 7). Consistent with the cyst excretion patterns, C57BL/6J mice exhibited very low trophozoite burdens at all time points; notably, at 6 months post-infection, only 1 out of 4 mice tested positive. Nevertheless, low-level infections
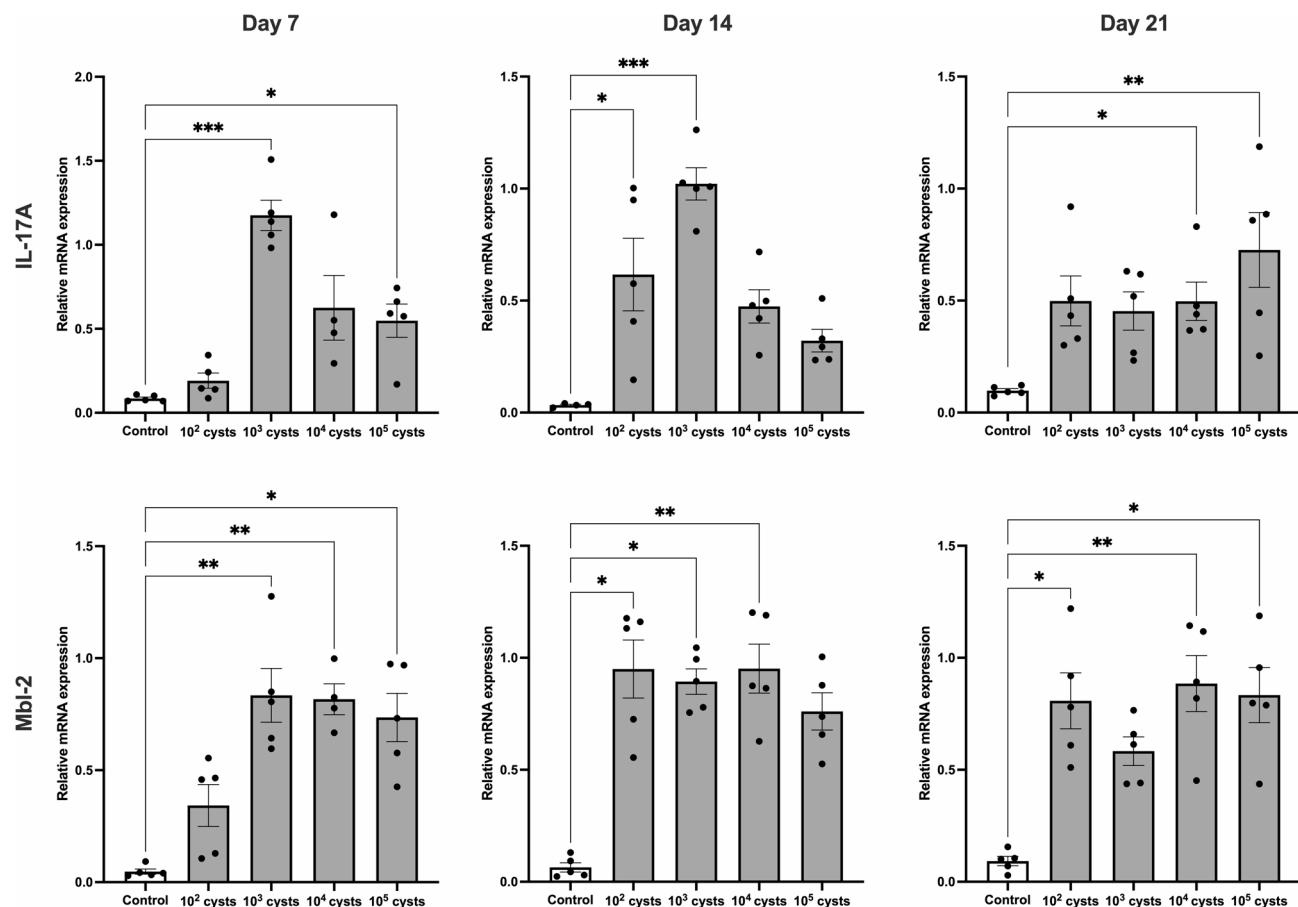
Fig. 3. IL-17A and Mbl-2 expression in the SI of *G. muris*-infected C57BL/6J mice across different infection doses. Relative mRNA expression levels of IL-17A and Mbl-2 in the SI were quantified by RT-qPCR at days 7, 14, and 21 p.i. (*n* = 5 per time point per group). Bars represent mean expression levels ± SEM. Differences were analyzed using a Kruskal–Wallis test (*$P < 0.05$, **$P < 0.01$, ***$P < 0.001$).
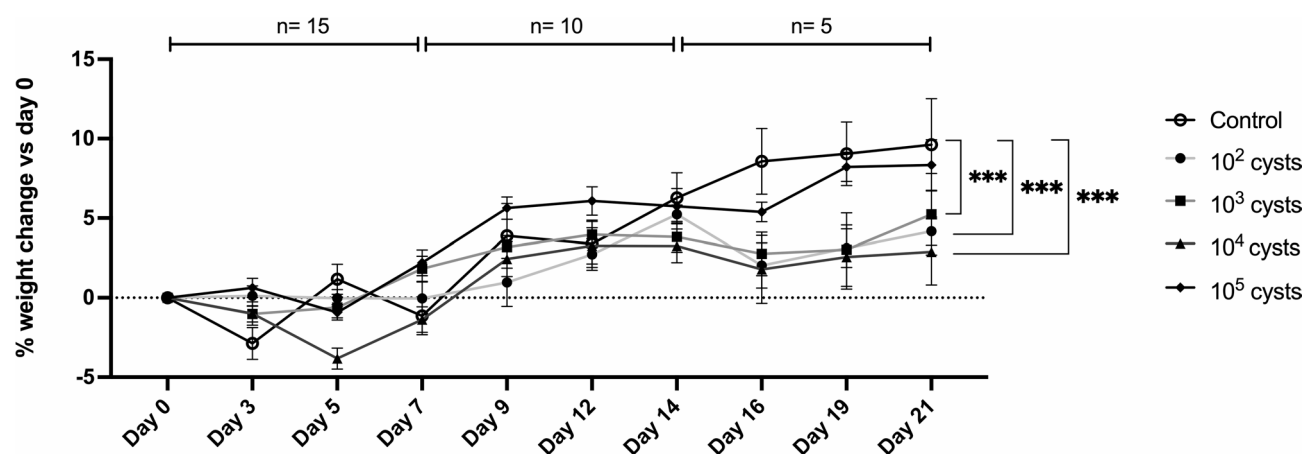
Fig. 4. Weight change in *G. muris*-infected C57BL/6J mice across different infection doses. Percentage weight changes relative to baseline (day 0, prior to infection) was monitored every 2–3 days until day 21 p.i.. Each point represents the mean percentage change in body weight ± SEM for each dose group. Statistical differences were analyzed using a linear mixed-effects model with mouse identity as a random intercept (*$P < 0.05$, **$P < 0.01$, ***$P < 0.001$).

a

b
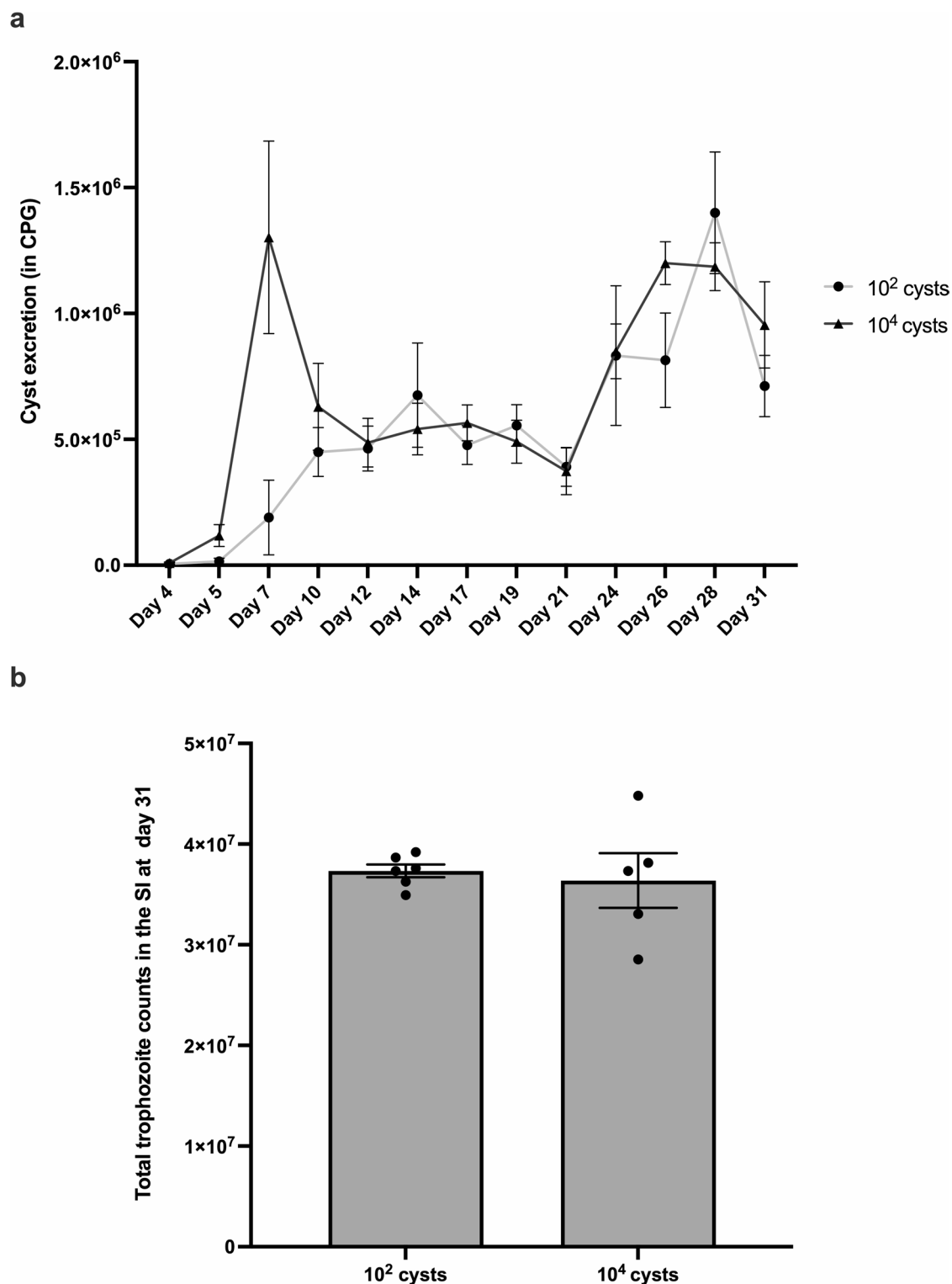
Fig. 5. Dose-dependent effects of *G. muris* infection on cyst excretion and intestinal trophozoite burden in TKO mice. (**a**) Fecal cyst counts were monitored every 2–3 days until day 31 p.i.. Each point represents the mean number of cysts per gram of feces (CPG) $\pm$ SEM ($n = 5$ per group). (**b**) Total trophozoite counts in the SI were quantified at day 31 p.i. ($n = 5$ per group). Bars represent mean values $\pm$ SEM. Differences between groups were assessed using a Kruskal–Wallis test.
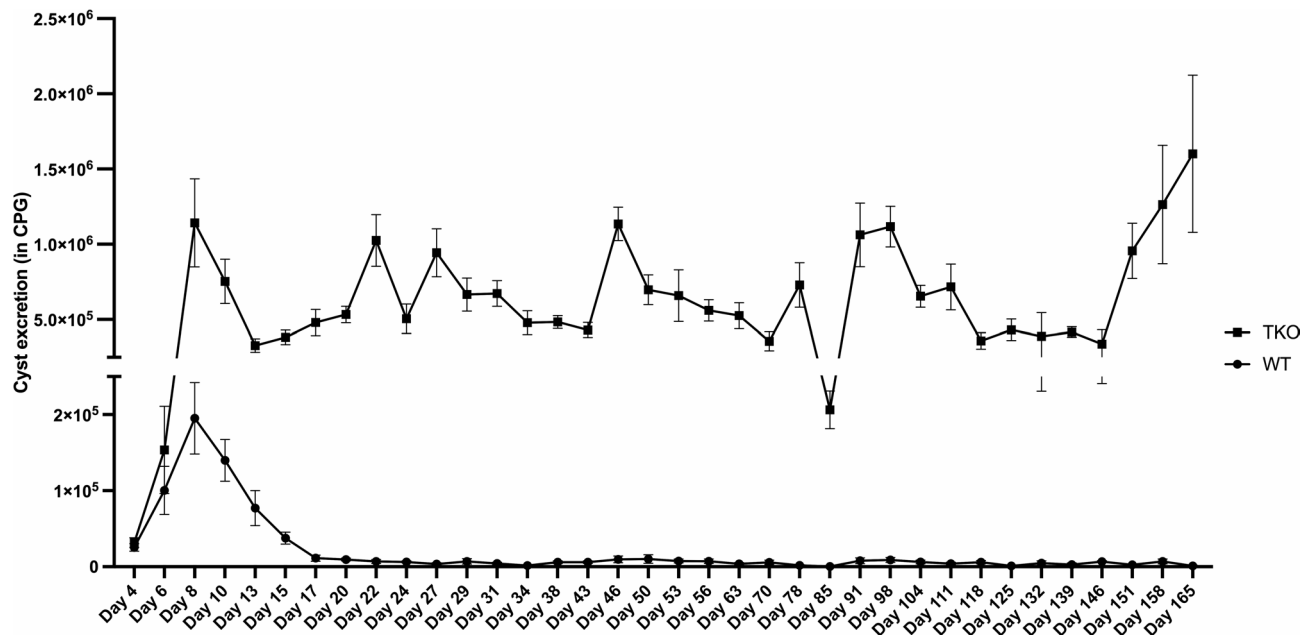
Fig. 6. Longitudinal monitoring of fecal cyst excretion in *G. muris*-infected C57BL/6J and TKO mice. Fecal cyst counts were recorded every 2–3 days during the first month p.i. (*n* = 12 per group), twice weekly from 1 to 2 months p.i. (*n* = 12), and weekly from 2 to 6 months p.i. (*n* = 8 for 2–4 months; *n* = 4 for 4–6 months). Each point represents the mean number of cysts per gram of feces (CPG) ± SEM.

below the calculated detection limit of 7,407 trophozoites per intestine cannot be excluded. In contrast, TKO mice maintained persistently high trophozoite counts throughout the study.

To assess the long-term effects of *Giardia* infection on the immune system, the expression level of IL-17A was assessed in both C57BL/6J and TKO mice at 2, 4 and 6 months p.i.. IL-17A expression was still clearly elevated at 2, 4 and 6 months after *Giardia* infection, reaching significance at 4 months p.i. (Fig. 8). No infection-related IL-17A upregulation was detected in TKO mice (**Supplemental Figure S3**). In a next step, several IL-17A downstream related targets were investigated. As mice without T cells could not produce significant amounts of IL-17A, TKO mice were not included in further gene analyses. Expression levels of Mbl-2, Ang-4, defensin-α−22 (Defα−22) and defensin-β−1 (Defβ−1) were quantified in the SI of C57BL/6J mice. The inclusion of Ang-4 and the defensins was based on the work of Paerewijck et al.[22], who reported significant upregulation of these antimicrobial peptides in *Giardia*-infected wild-type mice. Additionally, the macrophage-associated genes NOS2, arginase-1 (Arg1) and CX3C motif chemokine receptor 1 (CX3CR1) were investigated, as previous studies have reported intestinal macrophage infiltration and increased macrophage-associated marker expression during *Giardia* infection[31,32]. The expression of Mbl-2 remained at a high level throughout the whole 6-month study period, reaching significance at 2 and 6 months p.i.. Similarly, NOS2 expression was significantly elevated at 2 months p.i., and although not statistically significant at later timepoints, NOS2 remained consistently higher than in uninfected control animals (Fig. 8). In contrast, the expression levels of the antimicrobial peptides Ang-4, Defα−22, Defβ−1 and macrophage markers Arg1 and CX3CR1 did not differ between infected and control mice at any time point after infection (**Supplemental Figure S4**).

Discussion

The dynamics of a *Giardia* infection are shaped by a complex interplay between host immunity, parasite factors and environmental conditions. Among these, infection dose and host immune competence play a central role in determining the kinetics of parasite expansion, symptom severity and eventual control of the infection. Although early murine studies laid the foundation for understanding the dynamics of *G. muris* infections[26,29,30], this work predated the identification of IL-17A as a central cytokine in the host response to giardiasis and these investigations were limited to short-term observations. In the present study, we revisit the dose-dependent nature of *Giardia* infection in both immunocompetent and T cell-deficient mice, linking parasite burden and infection kinetics to IL-17A-mediated responses. Furthermore, we extend these findings through long-term longitudinal analysis, providing new insights into the chronic phase of infection and immune activation over time.

In line with early work by Roberts-Thomson et al.[29] and Belosevic et al.[30], we observed that higher inocula in C57BL/6J mice resulted in earlier cyst excretion, while lower doses led to delayed shedding. Interestingly, unlike the earlier studies which reported a similar peak of cyst output regardless of the initial dose, our data showed that the magnitude of the peak was dose-dependent: mice receiving the highest dose exhibited a sharp and pronounced peak around day 5–7 p.i., whereas lower-dose groups exhibited a more flattened and extended excretion profile. Despite these kinetic differences, cumulative cyst counts over the course of infection at day
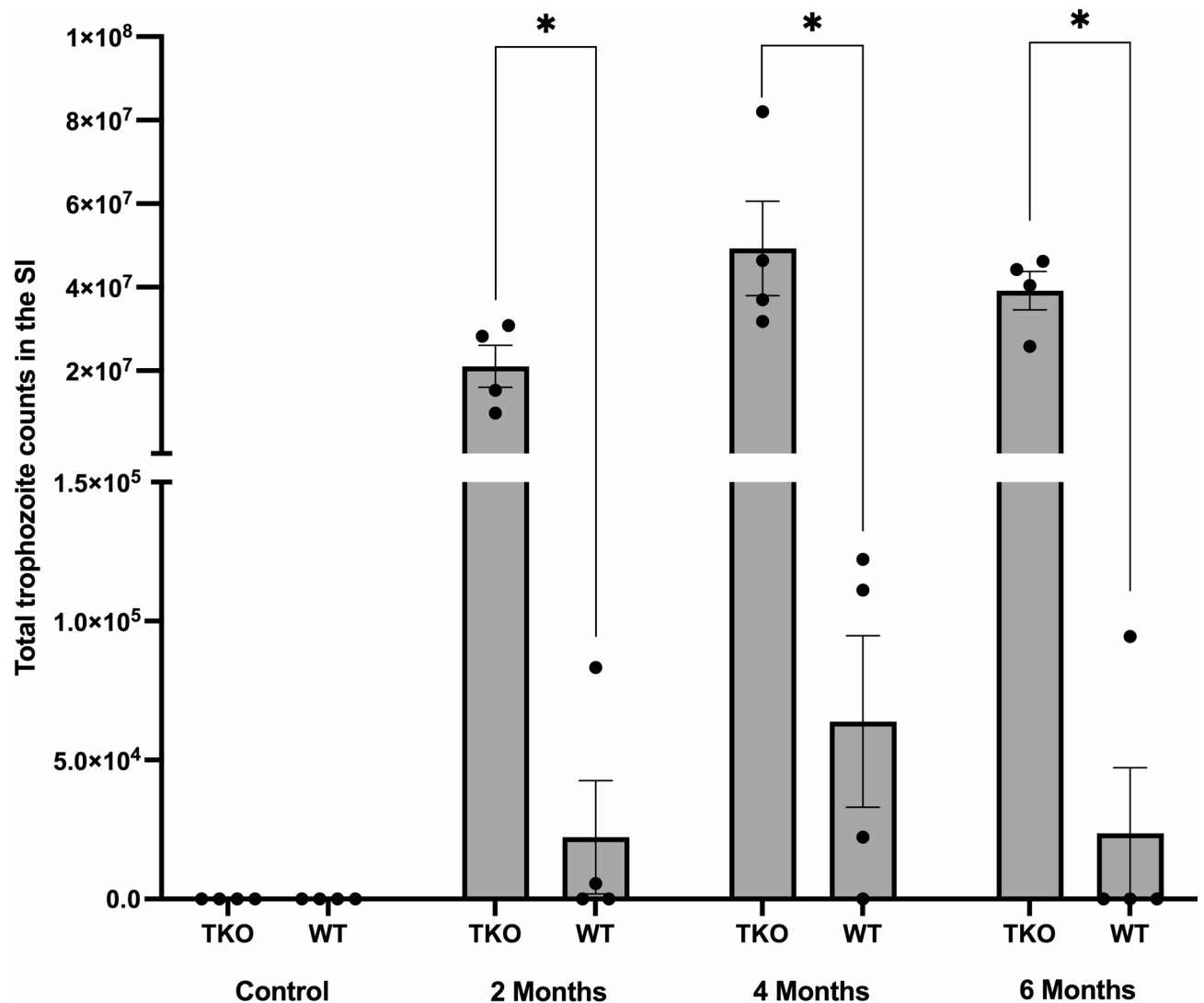
Fig. 7. Intestinal trophozoite burden in *G. muris*-infected C57BL/6J and TKO mice during chronic infection. Total trophozoite counts in the SI were quantified at 2, 4, and 6 months p.i. ($n = 5$ per breed per time point). Bars represent mean values ± SEM. Differences were analyzed using a Mann-Whitney test (*$P < 0.05$).
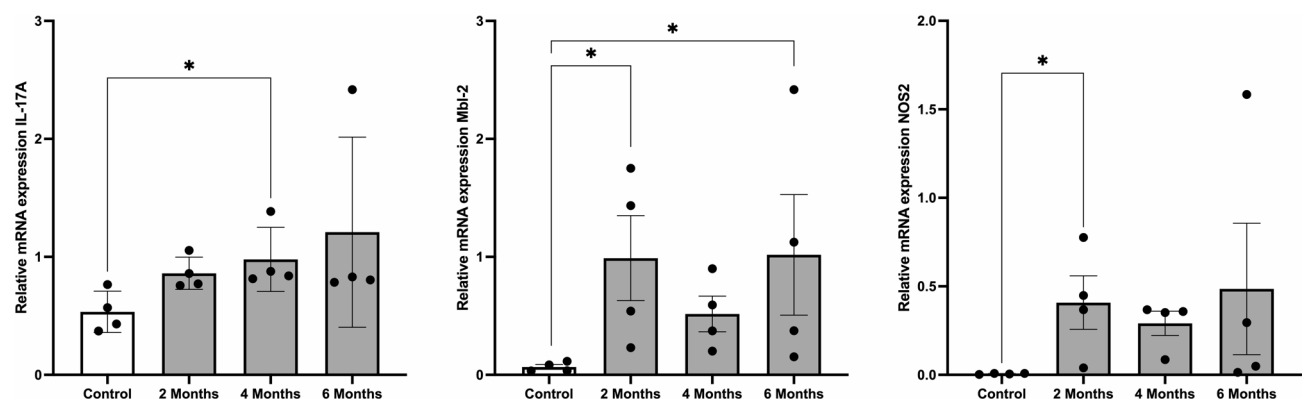
Fig. 8. IL-17A, Mbl-2, and NOS2 expression in the small intestine of chronically *G. muris*-infected C57BL/6J mice. Relative mRNA expression levels of IL-17A, Mbl-2, and NOS2 were quantified in the SI by RT-qPCR at 2, 4, and 6 months p.i. ($n = 4$ per time point). Bars represent mean expression levels ± SEM. Differences were analyzed using a Kruskal–Wallis test (*$P < 0.05$).

8

21 p.i. were comparable across all groups, indicating that total cyst shedding was ultimately independent of the initial dose. Consistent with this, cyst output and trophozoite burdens converged across all dose groups to a low level by day 21 p.i., reflecting an effective and timely control of *Giardia* infection regardless of the initial load. Interestingly, the lowest dose group showed more persistent cyst shedding and higher trophozoite counts specifically at day 14 p.i. compared to mice infected with higher doses, whose counts were already declining. This suggests that low-dose infections may initially evade host detection. However, because *Giardia* replicates exponentially by binary fission, this evasion is likely limited in time, as parasite numbers quickly reach a threshold that triggers host responses.

The decrease in parasite burden over time in the different groups coincided with IL-17A upregulation in the SI. IL-17A levels in the lowest dose group were only increased by day 14 p.i., while in the highest dose group, IL-17A was significantly elevated at day 7 p.i. and already decreased by day 14 p.i.. Despite this earlier induction, overall IL-17A expression levels in the highest dose group were lower compared to the lower dose groups. This likely reflects an earlier peak in IL-17A expression in the highest dose group that occurred prior to our first sampling point at day 7 p.i.. These findings confirm prior observations of the central role of IL-17A in murine giardiasis[19,22,33] and further suggest a possible trophozoite threshold for activating the protective Th17 immune response. This supports the idea proposed by Roberts-Thomson et al.[29] that larger inocula may generate a stronger antigenic stimulus earlier during infection, thereby accelerating immune activation and parasite elimination. Mbl-2, a key downstream effector, showed an extended induction pattern until the last time point after infection, consistent with its role in anti-giardial defence mechanisms[22].While the PP did not exhibit significant IL-17A upregulation in any dose group, Mbl-2 expression was increased at multiple time-points after infection in all dose groups. This suggests a possible involvement of the PP in anti-giardial immunity and should be further explored. In line with previous reports, the MLN showed no transcriptional activation of IL-17A, reinforcing the localized nature of the intestinal immune response to *Giardia* infection[19].

Body weight patterns in the different dose groups further reflected the complexity of host-parasite interactions. While Roberts-Thomson et al.[29] reported a dose-dependent impairment in weight gain, most pronounced at the highest inoculum, we observed that the highest-dose group did not show growth impairment, whereas the 3 lower doses were all associated with significantly reduced weight gain. A possible explanation for this is that the early robust immune response and rapid parasite control in the highest dose group may have limited inflammation, minimizing metabolic disruption and subsequent malabsorption and weight loss[34].

To investigate whether infection dose influences parasite dynamics in the absence of T cell-mediated immunity, TKO mice were infected with 10^2 or 10^4 cysts and the 2 dose groups were monitored for 31 days p.i.. Interestingly, despite this initial difference in inoculum size, the cyst output between the 2 groups converged within two weeks p.i.. In line with this, trophozoite numbers in the SI were comparable between the two groups at day 31 p.i.. This plateau in colonisation suggests that intestinal expansion of *Giardia* is self-limiting, even in the absence of immune-mediated control, probably due to host-intrinsic factors, such as limitations in epithelial binding sites or nutrient availability. In this experiment, TKO mice showed a secondary burst of cyst excretion around days 26–28 p.i., a pattern reminiscent of the intermittent or relapse-like shedding described in human giardiasis[35,36]. Such variations in cyst output, often accompanied by symptom fluctuations, are well documented in longitudinal clinical observations, particularly in immunocompromised patients[37,38]. This parallel suggests that impaired T-cell–mediated control may allow low-level parasite persistence followed by episodic expansion, mirroring patterns seen clinically.

It is well established that TKO mice are unable to clear *Giardia* infections within the typical three-week period, due to the absence of T cell-mediated immunity[19,20,25–27]. However, no previous studies have extended observations beyond 3 months p.i.. In the present study, TKO mice were monitored for 6 months after infection. As expected, the TKO mice were unable to control the infection and continued to excrete cysts throughout the entire 6-month observation period, suggesting that no alternative innate immune mechanisms are able to take over from T cells and control the infection.

To further explore the long-term immunological consequences of *Giardia* infection in immunocompetent mice, C57BL/6J mice were monitored until 6 months after infection. This longitudinal follow-up revealed that C57BL/6J mice did not eliminate the parasite from their intestine completely but maintained low-level fecal cyst excretion throughout the whole study period. Although trophozoite counts remained low during the chronic time points, there was sustained elevation of IL-17A, Mbl-2 and NOS2 after infection, suggesting prolonged mucosal immune activation. While NOS2 expression remained elevated after infection, the expression of other macrophage markers Arg1 and CX3CR1 remained unchanged. Given that NOS2 is not exclusively produced by macrophages and can also be expressed by epithelial and other non-myeloid cells[39], the observed expression was likely not macrophage related. Antimicrobial peptides such as Ang-4 and defensins were also not differentially expressed, suggesting that chronic IL-17A signalling may selectively maintain certain effector pathways. This diverges from the acute response, where a wider range of antimicrobial genes is typically induced[22]. Recently, Sardinha-Silva et al.[40] reported that *G. duodenalis* GS/M drives a type-2/IL-10 mucosal response in mice, with expansion of IL-10–producing Th2 cells at day 7 p.i. In contrast, our *G. muris* model shows a sustained IL-17A/Mbl-2/NOS2 signature. While species/strain differences are a plausible explanation, methodological variables (inoculum, sampling times, microbiota, housing) may also contribute. Given that multiple prior studies from different labs identify IL-17A–dependent mechanisms as central to parasite clearance while Th1/Th2 pathways are not essential for control, we focused this study on IL-17A and its downstream effectors[19,20,22,23,27,33,41,42].

In conclusion, this study connects classical murine models of giardiasis with current understanding of mucosal immune responses. While earlier work established the influence of infection dose, our findings clarify these concepts by linking them to IL-17A signalling and its downstream effector pathways. Infection dose impacts the timing and magnitude of the immune activation, but not the eventual control of the parasite. Additionally, sustained IL-17A-related gene expressions in wild-type mice after acute infection points to prolonged mucosal

immune activation, which may have dual consequences. On the one hand, it could contribute to possible long-term sequelae of *Giardia* infection, such as inflammatory bowel disease[6,34,43] and irritable bowel syndrome[44–46]; on the other hand, sustained immune activation could provide enhanced protection against secondary intestinal infections[15–18].

Methods

Ethical statement
All animal experiments were conducted in accordance with the European Union (E.U.) Animal Welfare Directives, the International Cooperation on Harmonization of Technical Requirements for Registration of Veterinary Medicinal Products (VICH) and the ARRIVE guidelines for reporting animal research. Guidelines for Good Clinical Practice and ethical approval to conduct the studies were obtained from the Ethical Committee of the Faculty of Veterinary Medicine, Ghent University (ethical committee approval numbers EC2023-085 and EC2024-033).

Mouse studies
All mice were obtained from Jackson Laboratories, acclimatized for one week upon arrival, and infected at six weeks of age. A total of three studies were conducted.

In infection study 1, 15 female C57BL/6J mice were infected with 10^2, 10^3, 10^4 or 10^5 cysts. A total of 15 uninfected mice were included as negative controls, with five animals euthanized at each timepoint. Cyst counts were performed every 2–3 days. At days 7, 14, and 21 p.i., five mice were euthanized to collect tissue samples to determine TCs and relative gene expression levels in the SI, PP and MLN.

In infection study 2, ten female B6.129P2-Tcr[btm1Mom] Tcrd[tm1Mom]/J mice (T cell knock-out, TKO), obtained from Jackson Laboratories, were used. Five mice were infected with 10^2 *G. muris* cysts and five with 10^4 cysts. Cyst counts were performed every 2–3 days. At day 31 p.i., all mice were euthanized and TCs were determined.

In infection study 3, fifteen female TKO and fifteen female C57BL/6J mice were infected with 10^3 cysts. An additional five uninfected controls were included for each strain. Cyst excretion was monitored for 6 months. Until one month p.i., cyst counts were performed every 2–3 days; from one to two months p.i., counts were performed twice weekly. Thereafter, cyst excretion was measured weekly until 165 days (6 months) p.i.. At 2, 4, and 6 months p.i., five mice per group were euthanized to determine TCs and collect tissue samples to determine relative gene expression levels in the SI. Mice from all three infection studies were euthanized by cervical dislocation.

Murine infection
Mice were infected with *G. muris* cysts delivered by oral gavage in 0.1 mL of distilled water. Infection doses varied according to the experimental design. The *G. muris* strain used in this study was originally provided by Dr. M. Belosevic (University of Alberta, Edmonton, Canada) and maintained by serial passage in CD1 mice.

Cysts were isolated from fecal pellets using a modified protocol based on Roberts-Thomson et al.[29]. Fresh feces were collected and suspended in 2 mL of bidistilled water and carefully layered over 8 mL of 1 M sucrose (specific gravity 1.11). Samples were centrifuged at $400 \times g$ for 15 min, after which the cyst-enriched interface was collected and pelleted by centrifugation at $800 \times g$ for 10 min. The resulting pellet was washed twice in 4 mL of distilled water ($800 \times g$ for 10 min). Following the final wash, cysts were resuspended in 1 mL of distilled water and concentrations were determined by enumeration in a hemocytometer.

Cyst counts
To monitor *G. muris* infection dynamics, cyst excretion was measured as previously described[25]. In summary, individual fecal samples were collected over a 2-hour period and weighed. Samples were homogenized in bidistilled water and centrifuged at $400 \times g$ for 15 min over a 1 M sucrose gradient. The cyst-containing upper layer was transferred to a clean tube and further washed by centrifugation at $800 \times g$ for 10 min. The supernatant was discarded, and the pellet was resuspended in 1 mL of bidistilled water. Cysts were counted using a haemocytometer and cyst excretion was expressed as cysts per gram of faeces (CPG).

Trophozoite counts
To quantify total small-intestinal trophozoite counts (TCs), the entire SI was dissected, opened longitudinally, and placed in 20 mL of phosphate-buffered saline (PBS). Tissues were incubated on ice for 15 min to facilitate detachment of trophozoites from the mucosal surface. The intestines were then vortexed thoroughly and trophozoites were counted using a haemocytometer (three technical counts per sample). Based on the total volume (20 mL) and the minimum detectable number of one trophozoite across three hemocytometer counts, the detection limit of this assay was calculated as 7,407 trophozoites per intestine.

Tissue sample collection
At necropsy, a 1-cm segment of the SI, beginning 4 cm distal to the gastroduodenal junction, was collected. When applicable (infection study 1), PPs along the entire SI were also collected and all MLNs were excised for further analysis. Tissues were snap-frozen in liquid nitrogen and stored at -80 °C for subsequent RNA extraction.

RNA isolation and quality control
Total RNA was extracted using the RNeasy Mini Kit (Qiagen), following the manufacturer's protocol. RNA quality was assessed using an Agilent Tapestation, and concentrations were measured with a NanoDrop ND-

1000 spectrophotometer (NanoDrop Technologies). Complementary DNA (cDNA) was synthesized using the iScript cDNA Synthesis Kit (Bio-Rad), according to the manufacturer's instructions.

Quantitative PCR (RT-qPCR)

Real-time quantitative polymerase chain reaction (RT-qPCR) was performed using SYBR Green Master Mix, following the protocol described by Dreesen et al.[33]. Primer sequences for all analysed genes can be found in **Supplementary Table S2**. Gene expression levels were normalized to the reference genes Hprt1 and Tbp, and relative expression was calculated using the ΔCt method[47]. Normalization of reference genes was performed using the geNorm algorithm[48].

Statistical analysis

All quantitative data are reported as the mean and standard error of the mean (SEM). Statistical analyses were performed using GraphPad Prism 10 (GraphPad Software) and RStudio (R version 2024.04.2; R Core Team). A one-tailed Mann-Whitney test was used for comparisons between two groups and a non-parametric Kruskal-Wallis test followed by a Dunn's multiple comparison test was applied to compare differences among more than two groups. For analyses involving multiple variables, Bonferroni's correction was applied to adjust for multiple comparisons. To evaluate the effect of infection dose on percentage weight gain over time, a linear mixed-effects model was fitted, with mouse identity included as a random intercept to account for repeated measurements within individuals. A P-value of < 0.05 was considered statistically significant.

Data availability

The datasets generated during and/or analysed during the current study are available from the corresponding author on reasonable request.

References

1. Lane, S. & LLoyd, D. Current trends in research into the waterborne parasite *Giardia*. *Crit. Rev. Microbiol.* **28**, 123–147 (2002).
2. Bernander, R., Palm, J. E. & Svärd, S. G. Genome ploidy in different stages of the *Giardia lamblia* life cycle. *Cell. Microbiol.* **3**, 55–62 (2001).
3. Adam, R. D. Biology of *Giardia lamblia*. *Clin. Microbiol. Rev.* **14**, 447–475 (2001).
4. Heyworth, M. F. Immunological aspects of *Giardia* infections. *Parasite* **21**, 55 (2014).
5. Rendtorff, R. C. The experimental transmission of human intestinal protozoan parasites. II. *Giardia lamblia* cysts given in capsules. *Am. J. Hyg.* **59**, 209–220 (1954).
6. Robertson, L. J., Hanevik, K., Escobedo, A. A. & Mørch, K. Langeland, N. Giardiasis - why do the symptoms sometimes never stop? *Trends Parasitol.* **26**, 75–82 (2010).
7. Escobedo, A. A., Hanevik, K., Almirall, P., Cimerman, S. & Alfonso, M. Management of chronic *Giardia* infection. *Expert Rev. Anti Infect. Ther.* **12**, 1143–1157 (2014).
8. Rishniw, M., Liotta, J., Bellosa, M., Bowman, D. & Simpson, K. W. Comparison of 4 *Giardia* diagnostic tests in diagnosis of naturally acquired canine chronic subclinical giardiasis. *J. Vet. Intern. Med.* **24**, 293–297 (2010).
9. O'Handley, R. M. et al. Duration of naturally acquired giardiosis and cryptosporidiosis in dairy calves and their association with diarrhea. *J. Am. Vet. Med. Assoc.* **214**, 391–396 (1999).
10. Gillon, J., Al Thamery, D. & Ferguson, A. Features of small intestinal pathology (epithelial cell kinetics, intraepithelial lymphocytes, disaccharidases) in a primary *Giardia muris* infection. *Gut.* **23**, 498-506 (1982).
11. Roxström-Lindquist, K., Palm, D., Reiner, D., Ringqvist, E. & Svärd, S. G. *Giardia* immunity - an update. *Trends Parasitol.* **22**, 26–31 (2006).
12. Daniels, C. W. & Belosevic, M. Comparison of the course of infection with *Giardia muris* in male and female mice. *Int. J. Parasitol.* **25**, 131–135 (1995).
13. Farthing, M. J. & Giardiasis *Gastroenterol. Clin. North. Am.* **25**, 493–515 (1996).
14. Mørch, K., Hanevik, K., Rortveit, G., Wensaas, K. A. & Langeland, N. High rate of fatigue and abdominal symptoms 2 years after an outbreak of giardiasis. *Trans. R Soc. Trop. Med. Hyg.* **103**, 530–532 (2009).
15. Kotloff, K. L. et al. Burden and aetiology of diarrhoeal disease in infants and young children in developing countries (the global enteric multicenter Study, GEMS): a prospective, case-control study. *Lancet* **382**, 209–222 (2013).
16. Hollm-Delgado, M. G. et al. Lack of an adverse effect of *Giardia intestinalis* infection on the health of Peruvian children. *Am. J. Epidemiol.* **168**, 647–655 (2008).
17. Muhsen, K., Cohen, D. & Levine, M. M. Can *Giardia lamblia* infection lower the risk of acute diarrhea among preschool children? *J. Trop. Pediatr.* **60**, 99–103 (2014).
18. Muhsen, K. & Levine, M. M. A systematic review and meta-analysis of the association between *Giardia lamblia* and endemic pediatric diarrhea in developing countries. *Clin. Infect. Dis.* **55** (Suppl 4), S271–293 (2012).
19. Dann, S. M. et al. IL-17A promotes protective IgA responses and expression of other potential effectors against the lumen-dwelling enteric parasite *Giardia*. *Exp. Parasitol.* **156**, 68–78 (2015).
20. Van Crombrugge, C. E., Decorte, B., Seys, L. J. M. & Geldhof, P. Unravelling the cellular sources and location of IL-17A production during a *Giardia* infection. *Sci. Rep.* **15**, 38790 (2025).
21. Iwakura, Y., Nakae, S., Saijo, S. & Ishigame, H. The roles of IL-17A in inflammatory immune responses and host defense against pathogens. *Immunol. rev.* **226**, 57–79 (2008).
22. Paerewijck, O. et al. Interleukin-17 receptor A (IL-17RA) as a central regulator of the protective immune response against *Giardia*. *Sci. Rep.* **7**, 8520 (2017).
23. Paerewijck, O., Maertens, B., Gagnaire, A., De Bosscher, K. & Geldhof, P. Delayed development of the protective IL-17A response following a *Giardia muris* infection in neonatal mice. *Sci. Rep.* **9**, 8959 (2019).
24. Li, E., Tako, E. A. & Singer, S. M. Complement activation by *Giardia duodenalis* parasites through the lectin pathway contributes to mast cell responses and parasite control. *Infect. Immun.* **84**, 1092–1099 (2016).
25. Roberts-Thomson, I. C. & Mitchell, G. F. Giardiasis in mice: prolonged infections in certain mouse strains and hypothymic (nude) mice. *Gastroenterol* **75**, 42–46 (1978).
26. Stevens, D. P., Frank, D. M. & Mahmoud, A. A. F. Thymus dependency of host resistance to *Giardia muris* infection: studies in nude mice. *J. Immunol.* **120**, 680–682 (1978).

27. Singer, S. M. & Nash, T. E. T-Cell-Dependent control of acute *Giardia lamblia* infections in mice. *Infect. Immun.* **68**, 170–175 (2000).
28. Roberts-Thomson, I. C., Stevens, D. P., Mahmoud, A. A. F. & Warren, K. S. Acquired resistance to infection in an animal model of giardiasis. *J. immunol.* **117**, 2036–2037 (1976).
29. Roberts-Thomson, I. C., Stevens, D. P., Mahmoud, A. A. & Warren, K. S. Giardiasis in the mouse: an animal model. *Gastroenterol* **71**, 57–61 (1976).
30. Belosevic, M. & Faubert, G. M. *Giardia muris*: correlation between oral Dosage, course of infection, and trophozoite distribution in the mouse small intestine. *Exp. Parasitol.* **56**, 93–100 (1983).
31. Fink, M. Y. et al. Proliferation of resident macrophages is dispensable for protection during *Giardia duodenalis* infections. *ImmunoHorizons* **3**, 412–421 (2019).
32. Maloney, J., Keselman, A., Li, E. & Singer, S. M. Macrophages expressing arginase 1 and nitric oxide synthase 2 accumulate in the small intestine during *Giardia lamblia* infection. *Microbes Infect.* **17**, 462–467 (2015).
33. Dreesen, L. et al. *Giardia muris* infection in mice is associated with a protective Interleukin 17A response and induction of peroxisome proliferator-activated receptor alpha. *Infect. Immun.* **82**, 3333–3340 (2014).
34. Hanevik, K. et al. Persisting symptoms and duodenal inflammation related to *Giardia duodenalis* infection. *J. Infect. Dis.* **55**, 524–530 (2007).
35. Ferreira-Sá, L. C. E., Machado, E. R., Gurgel-Gonçalves, R. & Abad-Franch, F. Disentangling the effects of intermittent faecal shedding and imperfect test sensitivity on the microscopy-based detection of gut parasites in stool samples. *PLoS Negl. Trop. Dis.* **18**, e0012719 (2024).
36. Halliez, M. C. & Buret, A. G. Extra-intestinal and long term consequences of *Giardia duodenalis* infections. *World J. Gastroenterol.* **19**, 8974–8985 (2013).
37. Lalle, M. & Hanevik, K. Treatment-refractory giardiasis: challenges and solutions. *Infect. Drug Resist.* **11**, 1921–1933 (2018).
38. Díaz-Alberola, I. et al. Incidence, management experience and characteristics of patients with giardiasis and common variable immunodeficiency. *J. Clin. Med.* **11**, 7007 (2022).
39. Korhonen, R., Lahti, A., Kankaanranta, H. & Moilanen, E. Nitric oxide production and signaling in inflammation. *Curr. Drug Targets Inflamm. Allergy.* **4**, 471–479 (2005).
40. Sardinha-Silva, A. et al. *Giardia*-induced type 2 mucosal immunity attenuates intestinal inflammation caused by co-infection or colitis in mice. *Nat. Microbiol.* **10**, 1886–1901 (2025).
41. Yordanova, I. A. et al. RORγt + Treg to Th17 ratios correlate with susceptibility to *Giardia* infection. *Scientific Reports.* **9**, 20328 (2019).
42. Maertens, B., Gagnaire, A., Paerewijck, O., De Bosscher, K. & Geldhof, P. Regulatory role of the intestinal microbiota in the immune response against *Giardia*. *Scientific Reports.* **11**, 10601 (2021).
43. Dann, S. M., Le, C. H. Y., Hanson, E. M. & Ross, M. C. Eckmann, L. *Giardia* infection of the small intestine induces chronic colitis in genetically susceptible hosts. *J. immunol.* **201**, 548–559 (2018).
44. Abedi, S. H. et al. The neglected role of *Blastocystis* sp. and *Giardia lamblia* in development of irritable bowel syndrome: A systematic review and meta-analysis. *Microb. Pathog.* **162**, 105215 (2022).
45. Hanevik, K. et al. Irritable bowel syndrome and chronic fatigue 6 years after *Giardia* infection: A controlled prospective cohort study. *Clin. Infect. Dis.* **59**, 1394–1400 (2014).
46. Litleskare, S. et al. Prevalence of irritable bowel syndrome and chronic fatigue 10 years after *Giardia* infection. *Clin. Gastroenterol. Hepatol.* **16**, 1064–1072e1064 (2018).
47. Livak, K. J. & Schmittgen, T. D. Analysis of relative gene expression data using real-time quantitative PCR and the 2(-Delta delta C(T)) method. *Methods* **25**, 402–408 (2001).
48. Vandesompele, J. et al. Accurate normalization of real-time quantitative RT-PCR data by geometric averaging of multiple internal control genes. *Genome Biology.* **3**, research0034.1-0034.11 (2002).

Author contributions
B.D., C.V.C. and P.G. conceived and designed the studies. B.D. performed the experiments with contributions of C.V.C. Data analysis was performed by B.D. The manuscript was written by B.D., C.V.C. and P.G. All authors read and approved the final manuscript.

Competing interests
The authors declare no competing interests.

Additional information
Supplementary Information The online version contains supplementary material available at https://doi.org/10.1038/s41598-025-32458-0.

Correspondence and requests for materials should be addressed to B.D.

Reprints and permissions information is available at www.nature.com/reprints.

Publisher's note Springer Nature remains neutral with regard to jurisdictional claims in published maps and institutional affiliations.